

Hazard Assessment for Pressure Tank Cars involved in Accidents

S. W. Kirkpatrick* and R.W. Klopp**

*Applied Research Associates, Inc., 830 E. Evelyn Ave., Suite C, Sunnyvale, CA 94086 USA

**Exponent Failure Analysis Associates, 149 Commonwealth Dr., Menlo Park, CA 94025 USA

Abstract - In the event of an accident or derailment involving a freight train, various personnel must respond to clear the right-of-way, repair the tracks, and remove the damaged rail cars. If the train contains pressure tank cars, the potential hazard needs to be assessed and safe handling procedures need to be followed. Since 1985, the Association of American Railroads, Transportation Technology Center (AAR/TTC) and other organizations have used a set of guidelines developed in the late 1970s to teach emergency response personnel how to make judgments in the field as to the severity of damage to tank cars involved in accidents. The severity of the damage then determines the appropriate course of action regarding rerailling, unloading, or moving the tank cars. Unfortunately, the Guidelines were developed by a few individuals who are no longer available to substantiate them. Thus, the guidelines lack validation beyond their reliable 15-year history and their level of conservatism is unknown. Fortunately, only very few catastrophic delayed ruptures have occurred, and those ruptures occurred in cases where the damage to the tank cars would not have passed the guidelines' rules.

A research program was begun to establish the validity of the Guidelines. The research program first focused on evaluating the technical foundation for the guidelines and the degree to which they have been validated. A program of experiments and analyses was then performed to validate the Guidelines and estimate their margins of safety. The experimental effort used small laboratory specimens to provide material property data as well as validation for the analyses. The structural and fracture mechanics analysis parts of the proposed research were accomplished by combining nonlinear finite element simulations with advanced elasto-plastic fracture and local fracture theories to quantify the severity of various types of tank car damage. The results of this research are being used to reformulate the Guidelines in more precise and quantitative terms, so that their use will contribute to increased safety at derailment sites. This paper describes the results of this program.

INTRODUCTION

In recent years there has been an ongoing research program sponsored by The U.S. Federal Railroad Administration (FRA) aimed at establishing guidelines (referred to here as "the Guidelines") for the proven and reliable assessment of damage to tank cars. The final objective of the project is to update the current handbook, Field Removal Methods for Tank Cars. This handbook helps emergency response personnel at an accident scene evaluate the criticality of damage to tank cars and, based on this evaluation, decide on the most appropriate procedures for handling the damaged cars and their contents (e.g., unload, reraill, or move the cars). The guidelines in this handbook have been used since 1985 by emergency response personnel to make judgments in the field as to the severity of damage to tank cars involved in accidents. Unfortunately, the Guidelines were developed by a few individuals who are no longer available to substantiate them. Therefore, a research program was begun to establish the validity of the Guidelines.

In Phase I of the program, research focused on evaluating the technical foundation for the Guidelines and the degree to which they have been validated. A literature review was performed to identify which of the current Guidelines can be validated with existing analyses and data and which require additional modeling and validation in a Phase II effort [1]. From the review of close to 100 references, analytical and experimental results were identified that can serve to evaluate the criticality of the damage (cracks, scores, gouges, dents, and wheel burns). The Guidelines were found to reflect a good overall, physical understanding of potentially dangerous damage to tank cars. Quantitative specifications of the damage are generally expressed in terms of convenient parameters that can be related to the degree of structural and material weakening caused by the damage. The following are conclusions from the Phase I study regarding the relevance and validity of the Guidelines.

- Little record of analytical or experimental work to support and validate the specifications of the Guidelines was found. However, some of the reasoning behind the specifications could be

reconstructed. It appears that the Guidelines rely on twenty-year old analysis methods and do not reflect recent advances in computational and fracture mechanics.

- The effect of loads applied to move or lift the derailed tank car is not explicitly accounted for in the Guidelines, even though these loads could be important in causing damaged areas to rupture.
- The margins of safety for specifications of the current Guidelines are not known.

Although the Guidelines lack formal validation, numerous documents provide informal validation. Training notes for damage assessment courses at AAR [2] provide rationale behind the Guidelines, but these notes are not readily available. Pellini's post-accident analyses [3-8] refer to and make numerous comments about the Guidelines. In general, these documents are supportive of the Guidelines as they exist.

Pellini's analyses are largely based on the so-called Slide-Graph Fracture Analysis System (SGFAS) [6]. Pellini used SGFAS to develop guidelines for the fracture-safe [7] and fatigue-reliable [8] design of steel structures. Pellini used the SGFAS to explain the good safety record of tank cars and the few occurrences of arrested or catastrophic brittle fracture (in particular, the two known cases [3,9] of catastrophic delayed fracture in tank cars containing extensive rail burn damage). Fracture safety evaluations with the SGFAS are made by entering into a graph the service temperature relative to the nil ductility temperature (NDT) and the normalized service stress. The location of this data point will fall either in a fracture arrest or a fracture propagation zone on the graph, and the tank car would be expected to behave accordingly. This procedure is simple and requires very little stress analysis because, in most reviewed references, the service stress is taken as either the membrane hoop stress induced by the tank internal pressure or the yield stress of the tank steel. It also avoids the difficulties of dealing explicitly with fracture in the transition region and under elastic-plastic or fully plastic conditions.

SGFAS is therefore a useful engineering design tool, even though it is somewhat qualitative and is based on fracture experience and theories dating back to the early 1970s. Since then, several significant advances have been made in the field of fracture mechanics that can be applied to the assessment of damaged tank cars. In particular, J-integral based elastic-plastic fracture mechanics and more recently developed damage mechanics or local fracture mechanics approaches can provide a more accurate estimate of the safety of a damaged tank car. In nearly all cases, these latter two approaches predict higher allowable pressures for a given level of damage.

The Guidelines' reliable 15-year history is, in itself, partial validation, but the level of conservatism is unknown. Fortunately, only very few catastrophic delayed ruptures have occurred, and those ruptures occurred in cases where the tank damage would not have passed the Guidelines' rules. No cases have been identified in which tanks have passed the Guidelines yet failed catastrophically.

From the recommendations of the Phase I program, a Phase II effort was performed to address the highest priority issues. The program objective was to validate the Guidelines, estimate their margins of safety, and develop an analysis method for generating a damage evaluation handbook. The structural and fracture mechanics analysis parts of the Phase II research was accomplished by combining nonlinear finite element simulations with advanced elasto-plastic fracture and local fracture theories to quantify the severity of various types of tank car damage. This analytical effort was performed in conjunction with an experimental effort using small laboratory specimens that provided material properties data as well as validation for the analyses. The remainder of this paper presents results of the Phase II research program.

TANK CAR STRUCTURAL ANALYSES

A finite element model of a DOT 112A340W pressure tank car was generated to analyze the loads and stresses in the tank car as a result of service and salvage operating conditions. The DYNA3D finite element code was used for the tank car modeling described in this paper. DYNA3D, developed at Lawrence Livermore National Laboratory [11], is an explicit nonlinear three-dimensional finite element code for analyzing the large deformation dynamic response of solids and structures.

Because the model is generated for the nonlinear dynamic finite element code DYNA3D, the model could also be used to calculate damage due to an impact with another structure in derailment or collisions. DYNA3D has many features ideally suited to vehicle collisions. A large variety of sliding interface (contact-impact) algorithms are available for modeling external collisions.

Two external views of the tank car model are shown in Figure 1. The structure includes the tank with ellipsoidal heads, manway, stub sill, bolster, and bogie structures. Figure 1b gives a detailed view of the model car end structures and the associated model mesh resolution. A pressure distribution on the inside of the tank and gravitational accelerations were used as boundary conditions to include the effects of the lading and pressure loads. The resulting simulations were used to investigate the effects of service and salvage loading on the stresses in the tank wall that could lead to an unstable tank rupture. In addition, the tank car model was used to calculate the behavior of dents in a tank car caused by impact in combination with the internal pressure. The results of these analyses are presented in the following sections.

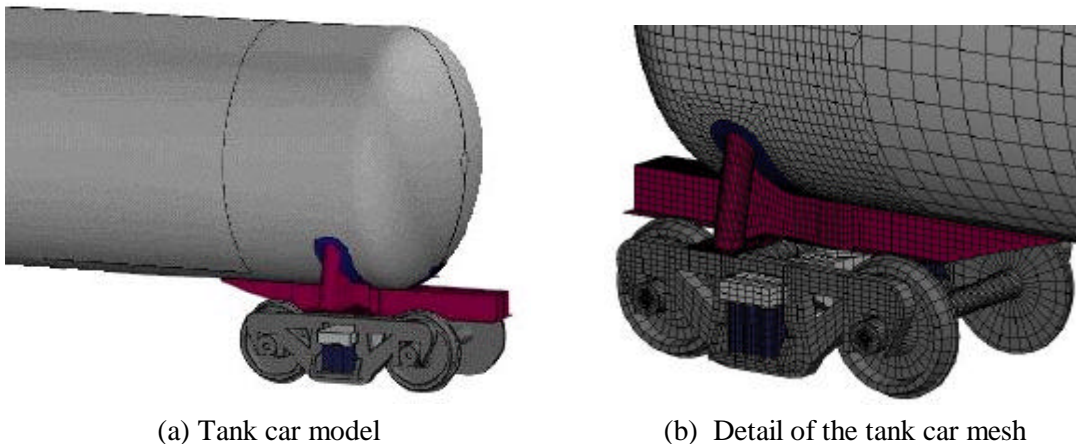


Figure 1. Model generated for a 112A340W pressure tank car.

Effects of Lifting Methods and Pressurization

The initial calculations with the tank car model were performed to determine the tank wall stress magnitudes from service and salvage loading conditions. For these simulations, the tank car is in an undamaged condition. A pressure distribution was specified on the inside of the tank wall to simulate the combined effects of an internal pressure and the hydrostatic pressure from the lading. In addition, a gravitational acceleration was specified to include the dead weight loading of the tank car structure. The resulting simulations were used to determine the magnitude of the stresses under various conditions.

The first simulation corresponds to the loading conditions of an unpressurized tank with a lading load from a full tank of fluid of density equal to water. The model predicts stress concentrations around the bolster and stub sill doubler plate, but the majority of the tank wall has stresses below approximately 40 MPa.

These results are consistent with simple estimates that can be made approximating the tank car as a simply supported beam.

Additional simulations were performed combining the gravity loading with internal pressures of 900 kPa and 1.75 MPa. The addition of the internal pressure increases the stress in the majority of the tank wall to approximately 85 MPa and 170 MPa respectively. The model again predicts stress concentrations around the bolster and stub sill doubler plate and near the tank head corner. The high stresses in the tank head are probably not characteristic because the increased head thickness that is usually found in practice and would reduce the stresses was not included in the model.

The expected stresses for the pressure loading can be estimated from the simple formulas used to analyze pressure vessels and pipelines. From this simple approach, the maximum stress in the tank wall is the hoop stress equal to the pressure multiplied by the radius-to-thickness ratio. Using the tank car pressure of 900 kPa and the tank dimensions in this relationship gives a circumferential stress of 86 Mpa, which is consistent with the calculation results.

The above calculations show that the stresses induced by lifting are small relative to stresses induced by tank pressure for the undamaged tank. We would expect this conclusion to hold for damaged tank cars as well because the types of damage that we are considering are localized such that the tank maintains its undamaged shape. We caution, however, that the lifting stresses, no matter how small, are additive to the pressure stresses, and could put critical stresses over the rupture limit.

Effects of Tank Pressure on Dent Behavior

Additional calculations were performed with the tank car model to investigate dent damage and the interaction of the internal pressure with a dent. The concern is that the pressure in a tank car can push out the dent such that the final dent shape does not indicate the full extent of deformation in the tank wall. In addition, a tank car with dent damage could be at risk of further plastic deformation if the internal pressure within the tank were to increase during the salvage operation.

A series of simulations were performed using both vertical and longitudinal indentors. From the simulations, the longitudinal dent was found to be the more critical dent orientation in the presence of internal tank pressure. An example simulation is presented here that illustrates the effect of internal pressure on the dent response. The simulation is for a longitudinal pole indenter with an impact velocity of 18 m/s. For this simulation the indenter has a rigid pole impact nose with a radius of 8 cm and a length of 3.0 m. The ends of the indenter pole were rounded away from the tank to avoid localized damage from the impact of sharp corners at the ends of the dent. The model used in this simulation is shown in Figure 2. The indenter produces a dent with the primary axes in the longitudinal direction. The simulation performed calculates the dent formation for an unpressurized tank then smoothly increases the internal pressure to a maximum level of 1.75 Mpa.

The calculated response is shown in Figure 3. The formation of the dent is shown in Figure 3(a). For visualization, only one half of the tank car model is shown in the figure. The maximum dent depth is approximately 15 cm at the center in the unpressurized tank. However, as the tank car pressure is smoothly increased to 1.76 Mpa, the dent is pushed outward to the point where the original dent is no longer visible at the tank centerline. This final tank geometry is seen in Figure 3(b). Additional simulations indicate that a significant reduction in a longitudinal dent depth occurs for pressures greater than 689 kPa. As a result, the final dent geometry in a pressurized tank car may not be a good indicator of the full extent of deformation in the tank wall.

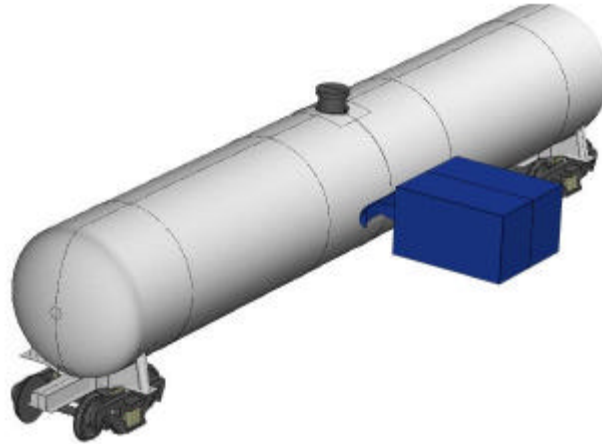
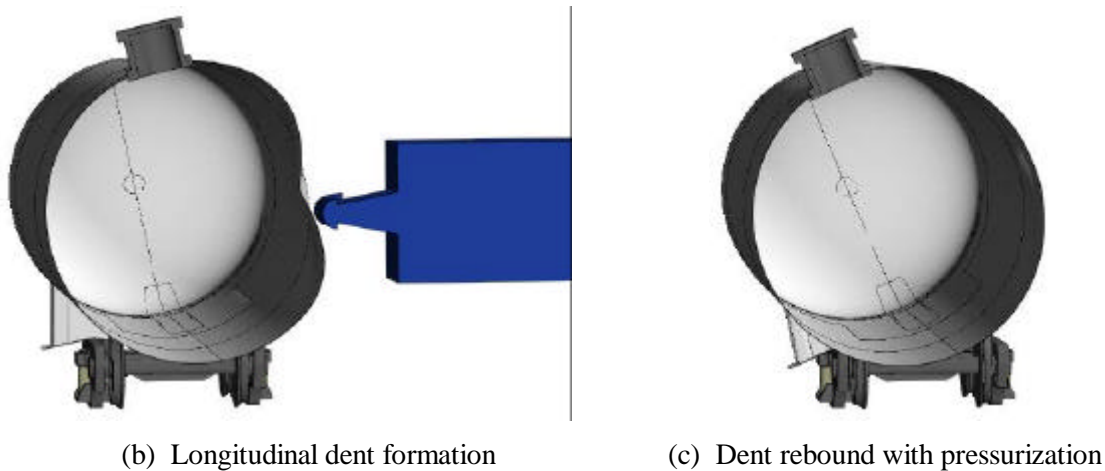


Figure 2. Model geometry for the dent formation and rebound simulations.



(b) Longitudinal dent formation

(c) Dent rebound with pressurization

Figure 3. Simulation of dent formation and rebound for a pressurized tank car.

Longitudinal Collision Response

A final impact simulation was performed with the tank car model to investigate impact conditions similar to that of the 112T340W tank car damaged in the May 25, 1995 Flomaton, AL collision. In that collision the tank car was impacted end-on by a locomotive. To approximate the collision a 120 Mg mass was impacted into the tank car end at 18 m/s. The tank car in the simulation was pressurized to 1.00 MPa.

The end-on impact response of the tank car is shown in Figure 4. The impact of the stub sill, tank end, and bogie against the rigid block produces damage that is mainly concentrated in the bolster and stub sill regions. The load on the sill and bogie produce a response that rotates the bolster away from the impact and forms a maximum dent in the tank approximately 1 meter behind the bolster location as seen in Figure 4 (b). The stub sill and doubler plate reinforce the tank structure such that the internal pressure does not significantly push the dent back out after the collision. This deformation mode and the location of the dent are similar to those observed in the Flomaton collision.

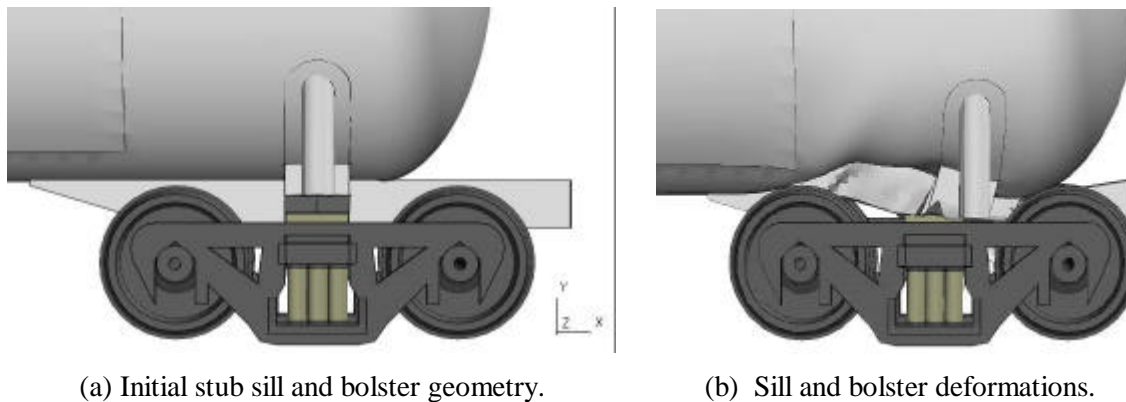


Figure 4. Collision damage for an axial impact against a rigid wall.

TANK FRACTURE ANALYSIS

The above structural simulations were very helpful in understanding the mechanisms that lead to collision damage in a tank car and in obtaining the stresses in the tank. The simulations identified the regions most critically stressed as well as the most severe loading configurations. However, the risk of a catastrophic failure of the tank for a given set of damage and loads still needed to be determined. The main objective of this research program was to apply advanced fracture mechanics analysis methods to obtain estimates of the risk of handling damaged tank cars.

Two key advances in fracture mechanics have occurred since Pellini's SGFAS. Both advances have resulted in more accurate and more general capabilities for modeling and predicting failure behavior. The first advance is the use of J-integral based elasto-plastic fracture mechanics (EPFM). Unlike SGFAS, EPFM can model cases when cracks are embedded in fully yielded regions, such as at the bottom of a rail burn dent. The second advance, brought into practice in the European nuclear industry, is the local fracture or damage mechanics approach. Unlike SGFAS and EPFM, the local fracture approach need not assume a preexisting macroscopic crack.

A significant safety hazard for damaged tank cars is produced by the weakening effect of burns, scores, gouges, dents or cracks located in the most critically loaded regions during an accident. Finite-element simulations of these regions can be performed with advanced fracture models to predict the onset of fracture in dents or at burns, scores, or gouges. Fracture experiments with small specimens of tank car steels (e.g., notched and cracked round bars, compact tension specimens, plates with simulated scores and gouges) provide the necessary experimental information for calibrating the fracture models and validating the simulation results.

The effect of dents on the structural integrity of tank cars can be conveniently assessed with structural analysis tools such as finite-element analysis. Linear elastic fracture mechanics or elasto-plastic fracture mechanics can evaluate the safety threat caused by the presence of cracks and can determine whether leak will occur before break. In contrast, burns, scores, and gouges present a more complex problem to which novel tools must be applied. This class of problem can be examined using the local fracture approach because it can, (1) predict fracture initiation in the absence of a preexisting macroscopic crack, (2) treat cases of multiaxial loading such as exist in a tank car, and (3) account for possible inhomogeneity in microstructure and properties. Therefore, we chose local fracture methodology as the core of our approach.

Of all the potential fracture modes in pressure tank cars, cleavage fracture presents the greatest risk. Cleavage cracks propagate with lower energy input, so results obtained are more conservative than for

tearing. On page 5 of his report on rail burns [3], Pellini makes the case that as-rolled steels then in service (1983) (and still in service today) are susceptible to cleavage fracture. He then presents several actual incidents that support his case. In none of the incidents were temperatures unusually low. In fact, some were in the 60°F range. Thus, we conclude that, although ductile tearing is a likely and preferred response, cleavage failure is a significant risk in any accident, and the Guidelines must allow that any fracture could result in cleavage.

The cleavage model used in our analysis is the local cleavage criterion developed by Beremin and coworkers [10]. The term “local criterion” describes a modeling approach in which damage is calculated locally within the material based on the stress and strain states using a micromechanical model for the fracture processes.

Predicting cleavage fracture is different from predicting most ductile damage processes in that there is typically a large scatter in the measured cleavage fracture stress for a sample of identical tests on a single batch of material. Thus a cleavage failure criterion will predict a probability of fracture for a given material, geometry, and stress level, rather than specify a deterministic failure stress.

The microstructural processes that produce a cleavage fracture are similar to many other classical fracture problems. The material is assumed to have a distribution of preexisting microcracks, typically initiated in the material from inhomogeneities. For example, in mild steels, the microcracks are produced by fracture of sulfide inclusions or grain boundary carbides. The catastrophic propagation of these cracks results in a cleavage fracture, which occurs when the stress normal to the microcrack planes reaches a critical value. This critical stress, s_c , can be approximated as

$$s_c = \left[\frac{2Eg}{p(1-\nu)l_o} \right]^{1/2} \quad (1)$$

where E is Young's modulus, g is the fracture surface energy, ν is Poisson's ratio, and l_o is the microcrack length.

The statistical nature of the cleavage criterion is introduced by the distribution of microcrack sizes within the material. Within a given microstructural characteristic volume (V_o), the probability of finding a crack of length between l_o and $l_o + dl_o$ is taken as

$$P(l_o)dl_o = \frac{a}{l_o^b} dl_o \quad (2)$$

By integrating the microcrack distribution function over the range of crack lengths greater than or equal the critical crack length at a given stress level, we obtain the probability of failure as

$$P(s) = \left(\frac{s}{s_u} \right)^m \quad (3)$$

where $m = 2b - 2$ and s_u is a material constant.

The remaining step in determining the cumulative failure probability of the structure is to combine the probabilities in each of the small representative volumes. Because the probability in any single representative volume is small, the cumulative rupture probability, P_R , can be approximated as

$$P_R = 1 - \exp \left[- \sum_j \frac{V_j}{V_0} \left(\frac{s_j}{s_u} \right)^m \right] \quad (4)$$

where the summation, j , includes all elements with nonzero plastic strain, V_j is the element volume, and V_0 is a characteristic microstructural volume. The above rupture probability function is used to estimate cleavage failure. Additional information about this model can be found in Reference 10.

The local fracture model for cleavage rupture was incorporated into the DYNA3D finite element model. To describe the modifications we made to DYNA3D, we first outline the solution procedure used in this code. DYNA3D is organized in a modular fashion, with each module performing a specific task. This procedure is common to most explicit finite element codes and is similar to those described by other authors (e.g., Owen and Hinton, [12]). The following simplified flow chart shows the tasks performed by DYNA3D. We will use this outline to describe where modifications to the code were made in the failure analyses.

Task 1: Input—Data are input to describe the geometry, materials, boundary conditions, loading, and solution control parameters.

Task 2: Initialize—Initial values read into the structural and material data arrays.

Task 3: Calculate nodal forces—Nodal forces are calculated as the difference between internal and external forces. External loading would include pressure, concentrated loads, and gravity. Internal forces are calculated from stresses.

Task 4: Solve equations of motion for accelerations—At each node, the acceleration is calculated from the force divided by the nodal mass. For explicit codes such as DYNA3D, no global stiffness matrix coupling the degrees of freedom is needed.

Task 5: Update velocities and displacements—Nodal velocities and displacements are calculated and updated by using accelerations and the current time step.

Task 6: Calculate strain increment—From the nodal velocities, strain rates are calculated from which strain increments can be calculated.

Task 7: Calculate element stresses—Element stresses are calculated in the material constitutive models from the strain increments.

Task 8: Calculate internal forces—Nodal internal forces are calculated by integrating the element stresses.

Task 9: Output and check for problem termination—Output results if specified. If the calculation time is less than the specified termination time, return to Task 3.

The code changes performed here to implement the Beremin cleavage model primarily take place in Task 7, in the routines where element stresses are calculated; however, other subroutines are also affected (such as material model input, summation of fracture probability, damage parameter output). The resulting model calculates a probability of fracture at each time step.

LABORATORY TESTING AND MODEL CALIBRATION.

Two series of laboratory tests were performed on the tank car materials of interest. The first series of material tests was performed using both smooth and notched round bar tensile specimens to provide fracture data required as input for the local fracture model. The second series of engineering tests was

performed to measure the fracture behavior on laboratory scale specimens. The results of these tests substantiate the guidelines as well as provide data to validate the local fracture model. These included both gouge specimens and bend specimens. The bend specimens were used to investigate damage produced by denting of the tank.

Two different tank car materials were tested, A515 Grade 70 and TC-128B in the as-rolled condition. The results presented in this paper are primarily for the tests on the A515 Grade 70 material. The A515 Grade 70 steel is a replacement for A212 Grade B steel, an obsolete specification that was withdrawn by ASTM in 1966. A comparison of the various tank car steels and the rationale for selecting the steels that were tested in this program are given in Reference 1. Roughly 15% of the current DOT 112 tank car fleet was built before 1966, when the A212 specification was in use. Most of these cars will be in service at least another decade and appear to represent the greatest risk of catastrophic rupture in accidents.

In choosing the temperature for the validation and calibration laboratory tests, we needed to satisfy three competing constraints. First, the tests must be performed at a low enough temperature that cleavage fracture, rather than ductile tearing, is ensured. Second, we should test at a temperature that fairly represents the most brittle conditions likely to be found in the field yet does not lead to overly conservative results. Third, the tests must be performed at a temperature that is practical to reach in the laboratory.

In the AAR literature on A212B/A515-70 as-rolled steel, we find that the lowest expected NDT is around -7°C . Unfortunately, the NDT is measured under dynamic conditions and in the presence of a weld. Our tests were performed under quasistatic conditions mostly without welds, and steels are generally less prone to cleavage under such conditions. Thus, to ensure that cleavage occurred, we had to test at a temperature well below the lowest expected NDT. We found it necessary to test smooth, macroscopically unflawed specimens at around -150°C to ensure that cleavage fracture occurred. Thus, we chose -150°C as the temperature for most of our testing. For these low temperature tests, specimens were either immersed in liquid nitrogen and cooled to -196°C , placed in the testing machine and allowed to warm to the desired temperature, then tested, or they were placed in an insulated box surrounding the grip area of the testing machine and liquid nitrogen was piped into the box until the desired temperature was reached.

A potential concern is that the results will be too conservative since temperatures of -150°C are never expected in the field. This concern can be eliminated, except perhaps for dents, because once typical tank car steels are cooled into the cleavage regime, the variation of fracture resistance with temperature can be predicted from knowledge of the variation of cleavage stress and flow strength with temperature. For a given steel, cleavage stress is relatively constant with changes in temperature. Thus, once we are in the cleavage regime, results are expected to be similar for all cases in which cleavage occurs. However, the flow stress rises with decreasing temperature, so results must be adjusted to take this into account. For example, if a gouge specimen cleaves under a certain stress at -150°C , we expect that, if cleavage were somehow initiated at a higher temperature, the cleavage stress would be nearly the same, although the strain necessary to reach that stress would be higher. We needed to verify, however, that the specimen would not first fail by ductile fracture at a lower stress due to the decreased flow stress at the higher temperature.

In the case of dents, if the tank steel is in the cleavage regime during dent formation, the tank will fail immediately. We showed this by performing cold bend tests at -150°C . TC-128B as-rolled, A515-70, and welded A515-70 plates all failed in cleavage at bend radii around 30 inches, far in excess of the 2-inch and 4-inch limits specified in the Guidelines. Apparently, if a dent is observed in a tank that has not ruptured, the dent was formed when the steel was in the ductile regime. Thus, to evaluate the validity of the dent guidelines, one must determine the subsequent behavior of the tank, particularly whether a delayed brittle rupture could occur.

Model Calibration and Validation

Smooth round bar tensile tests and calculations were performed at various temperatures to establish the stress-strain behavior of the steels and the increase in flow strength with decreasing temperature. The finite element model of the smooth round bar test specimen is shown in Figure 5. During the tests, a 25-mm gauge length extensometer was installed to record engineering strain. Posttest, failed neck diameters were measured to provide the final true strain for input to the finite element model. All tests were performed at approximately 10^{-3} s^{-1} strain rate.

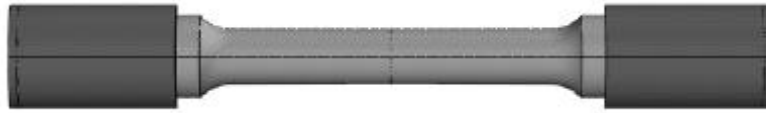


Figure 5. Finite Element Model of the smooth round bar tensile test specimen.

The smooth round bar tensile tests were performed on the A515-70 tank car steel at various temperatures ranging from 20°C to -160°C . The results of the coupon tests were used to calibrate the stress-strain behavior in the constitutive model. An estimate of the true stress-strain curve is first obtained from the measurement of the engineering stress-strain behavior and periodic measurements of the necking behavior. This true stress-strain behavior is input into the constitutive model in tabular form. Performing iterative simulations of the tensile test can further refine the true stress-strain curve by adjusting the material parameters until the necking behavior is accurately reproduced. The resulting measured and calculated engineering stress-strain curves for the A515-70 tank car steel at -150°C is shown in Figure 6.

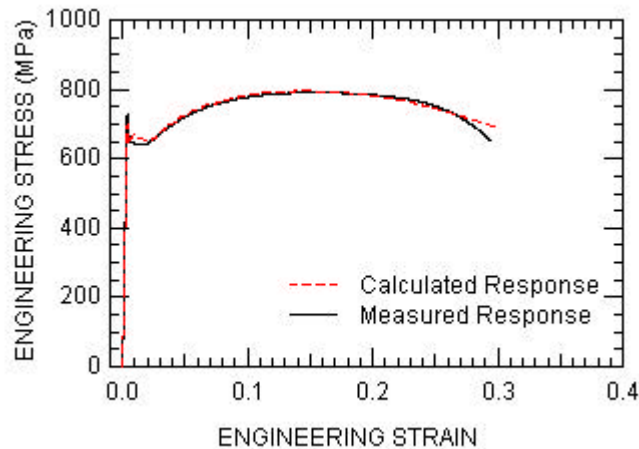


Figure 6. Measured and calculated behavior for the smooth round bar tensile test.

The next step is to use the stress-strain behavior from the smooth round bar to analyze the notched round bar specimens. The notched round bar tensile tests establish the stress-strain and fracture behavior of the steels under varying levels of triaxial constraint. Specimens were machined with three notch root radii: 6.35 mm, 2.54 mm, and 1.27 mm. Finite element models of the notched round bar tensile specimens were created as shown in Figure 7. Test data and analyses of these coupon tests were used to calibrate the Beremin cleavage fracture model for the two tank car materials. The finite element models of the tensile specimens had an element size of approximately $400 \mu\text{m}$ in the gauge section. With these simulations, the cleavage stress (σ_u) can be varied until a good match between predicted and measured rupture stresses is obtained. The microcrack exponent (m) was assigned a value of 22 based on results of previous studies [10].

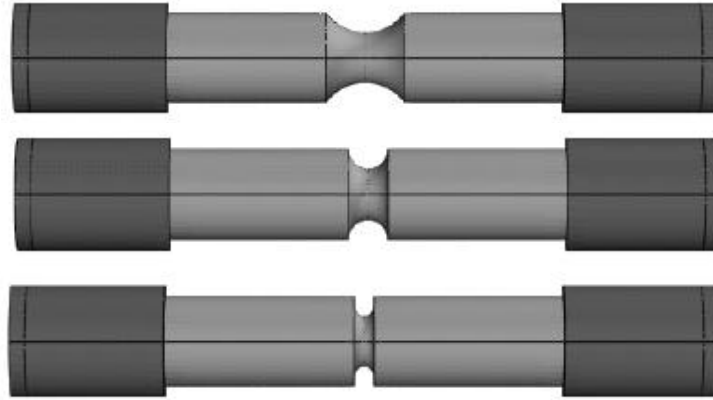


Figure 7. Finite Element Models of the notched round bar tensile test specimens.

During the notched round bar tests, a 25-mm gauge length extensometer was installed such that the gauge length straddled the specimen notch. The extensometer output was used to verify the displacement computed in the finite element model. In a few room temperature tests, a radial extensometer was also applied to measure the change in specimen diameter as necking proceeded. For the tests in the cleavage regime (-150°C), the radial extensometer was unnecessary because the amount of necking was insignificant. All tests were performed with a displacement rate of 25 $\mu\text{m/s}$.

For the given values of the cleavage model parameters, a probability of rupture can be determined at any load level. For the A515-70 steel a value of 1.65 GPa for the cleavage stress was used to fit the notched round bar data. The characteristic volume (V_0) was obtained as the cube of the characteristic microstructural length (200 μm). Figure 8 compares the resulting calculated notched round bar behaviors for the A515-70 steel with representative curves from tests. The load levels for 5%, 50%, and 95% rupture probability as obtained from the cleavage model are indicated in the figure.

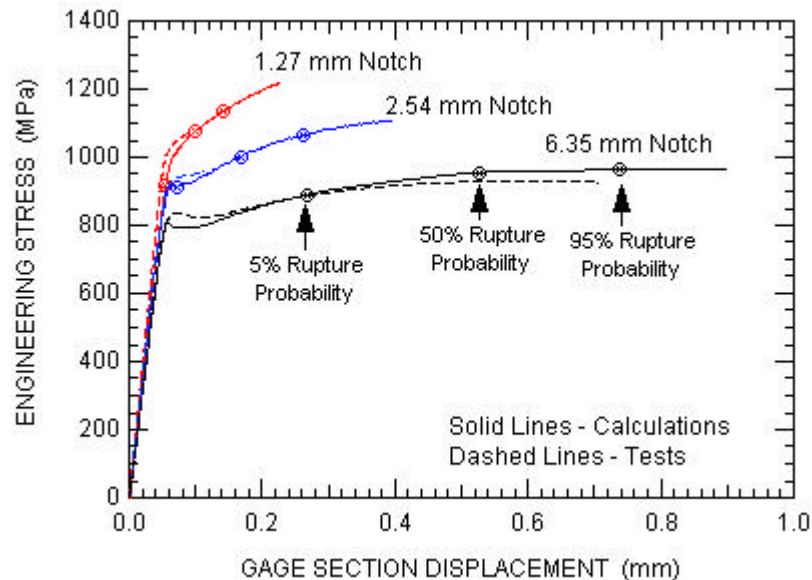


Figure 8. Measured and calculated behavior for the notched round bar tensile tests.

The statistical nature of cleavage fracture can be seen by normalizing all the notched round bar failure stresses by the predicted load level for a 50% probability of failure. These normalized failure stresses can then be plotted against a normalized rupture probability curve as shown in Figure 9 for all of the A515-70

steel tensile tests. This fit is good over the full range of tests performed considering the relatively small statistical sample of tests.

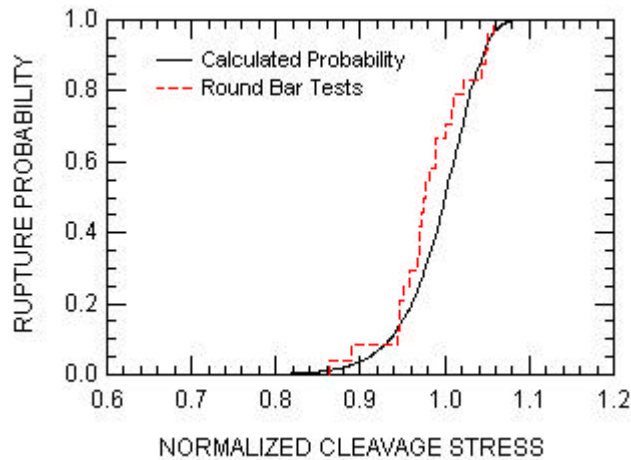


Figure 9. Measured and calculated behavior for the smooth round bar tensile test.

Engineering Test Models

As part of the engineering approach, we performed coupon tests with simulated gouges and bend bar tests to investigate dent damage. The results of the gouge specimen tests are presented here. These tests provided an opportunity to directly validate the gouge guidelines and to further validate the calibrated finite element models. A finite element model of an engineering gouge specimen is shown in Figure 10. The specimens all had the same width (44.5 mm), the same gouge depth (6.35 mm) and were of the as-rolled thickness, but had two different gouge root radii, 12.7 mm and 3.2 mm. All gouge tests were performed in the cleavage regime at a loading rate around 2.5 mm/s. Extensometers were installed on the front and back faces of the specimens, bridging the notches, to verify the displacements computed in the finite element models and to measure the amount of bending induced by the asymmetry of the specimen and loading.

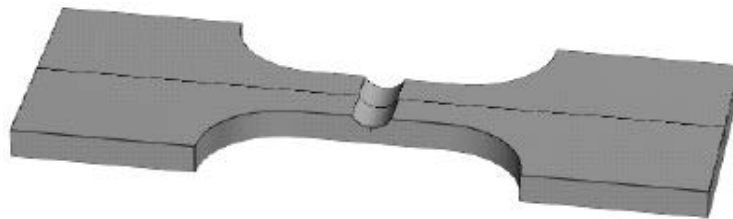


Figure 10. Finite Element Model of an engineering test gouge specimen.

Test data and analyses results of these engineering tests were used to validate the Beremin cleavage fracture model. The calculated and measured gouge test results for the A515-70 steel are summarized in Figure 11. The predicted load-displacement behavior for the bend tests agrees reasonably well with the measured values. The discrepancies between measured and predicted stress-displacement behaviors can be attributed to slight temperature variations between specimens and the small increase in temperature that occurs during the duration of experiment. The cleavage model does a good job of predicting the cleavage rupture of the gouge tests for the A515-70 steel. The greatest discrepancy is for the 0.5-inch-radius gouge, which appears to be more ductile than the calculated result. However, the measured cleavage stress of 486 MPa is below the calculated 95% rupture probability stress of 489 MPa. The additional ductility and lower stresses are a result of an increasing temperature of the specimen, a condition that was not included in the simulation.

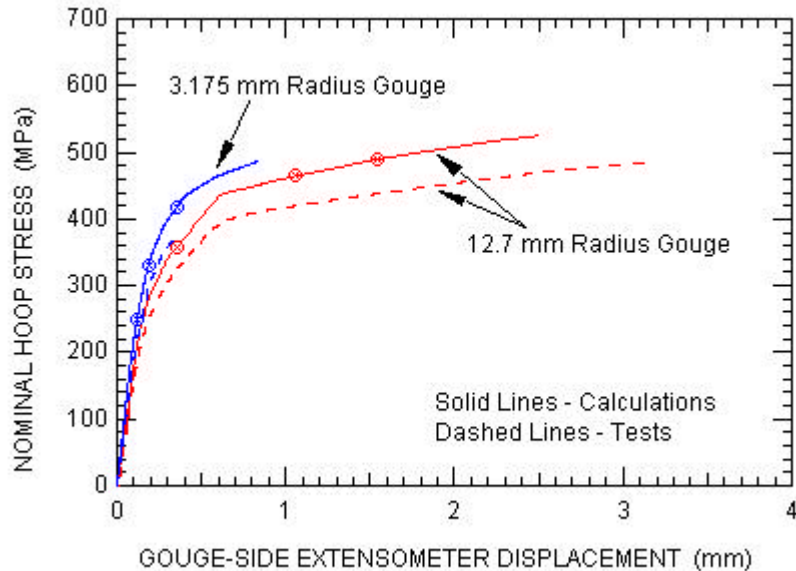


Figure 11. Finite Element Models of the engineering test gouge specimens.

CONCLUSIONS

The existing AAR Accident Damage Assessment Guidelines lacked formal validation. The Guidelines' reliable 15-year history provides some degree of validation, but the level of conservatism is unknown. Fortunately, only very few catastrophic delayed ruptures have occurred, and those ruptures occurred in cases where the tank damage would not have passed the Guidelines' rules.

To validate the Guidelines, a research program was performed combining laboratory tests and computer simulations. The approach was to focus on DOT 112A340W tanks and use laboratory tests on A515 Grade 70 and TC-128B as-rolled plate to calibrate a finite element and local cleavage fracture model. The resulting computational tool was helpful in analyses of tank damage and can be used to further analyze the Guidelines for other tank cars, damage scenarios, and salvage operations. The laboratory tests both provided data to validate the cleavage model and directly simulated damage in the form of gouges and dents.

The effect of rerailling and service loads on undamaged tank cars was investigated. The analyses found that rerailling stresses are small compared to pressure stresses for pressures of 690 kPa and above. Additional simulations were performed to investigate the interaction of internal pressure with dent formation. The calculations show that when internal pressures of 690 kPa or greater are present, significant rebound of the dent is likely. Therefore, the final dent geometry is not necessarily a good indicator of the total dent damage.

REFERENCES

1. Giovanola, J. H., and D. A. Shockey, "Literature Search and Evaluation Pertaining to Damage Assessment of Tank Cars Involved in Accidents," Phase I Final Report prepared for the Association of American Railroads Transportation Technology Center, Subcontract No. 940986 under Federal Railroad Administration Contract No. DTFR53-93-C-00001, Task Order 115, SRI International (Project 7483), Menlo Park, CA (October 1995).
2. Davis, J. C., AAR private communication (1997).
3. Pellini, W. S., "Analysis of Tank Car Failures Related to Rail Burn Dents," Association of American Railroads, Report No. R-551, Chicago, Illinois (June 1983).

4. Pellini, W. S., "Feasibility Analysis for Tank Car Applications of New Microalloyed and Controlled Rolled Steels—Description of Fracture Properties and Comparisons with Steels in Present Use," Association of American Railroads, Report No. R-543, Chicago, Illinois (April 1983).
5. Phillips, E. A., and W. S. Pellini, "Phase 03 Report on Behavior of Pressure Tank Car Steels in Accidents," Association of American Railroads, Report No. RA-03-6-48 (AAR R-553), Chicago, Illinois (June 20, 1983).
6. Pellini, W. S., "Slide Graph Fracture Analysis System," Association of American Railroads, Report No. R-552, Chicago, Illinois (June 1983).
7. Pellini, W. S., "Guidelines for Fracture-Safe Design of Steel Structures," Association of American Railroads, Report No. R-455, Chicago, Illinois (November 1980).
8. Pellini, W. S., "Guidelines for Fatigue-Reliable Design of Steel Structures," Association of American Railroads, Report No. R-490, Chicago, Illinois (September 1981).
9. National Transportation Safety Board, "Derailment of Louisville and Nashville Railroad Company's Train No. 584 and Subsequent Rupture of Tank Car Containing Liquefied Petroleum Gas Waverly," Railroad Accident Report No. NTSB-RAR-79-1, Notation 2313B, Washington, DC (February 22, 1978).
10. Beremin, F. M., "1983, "A Local Criterion for Cleavage Fracture of a Nuclear Pressure Vessel Steel," Metallurgical Transactions A, Vol. 14A, November, 1983, pp. 2277-2287.
11. Whirley, R. G., and B. E. Engelman, "DYNA3D—A Nonlinear, Explicit, Three-Dimensional Finite Element Code for Solid and Structural Mechanics—User Manual," Report UCRL-MA-107254 Rev. 1, Lawrence Livermore National Laboratory (November 1993).
12. Owen, D.R.J., and E. Hinton, *Finite Elements in Plasticity: Theory and Practice* (Swansen, United Kingdom, Pineridge Press, 1980).